Inhibition of aquaporin-4 significantly increases regional cerebral blood flow

Hironaka Igarashi[a], Mika Tsujita[a], Yuji Suzuki[a], Ingrid L. Kwee[b] and Tsutomu Nakada[a,b]

The effects of the aquaporin-4 (AQP-4) inhibitor TGN-020 on regional cerebral blood flow (rCBF) was examined in wild-type (WT) and AQP-4 knockout (KO) mice *in vivo*. Although baseline absolute rCBF of WT and KO mice were equivalent (158.9±17.7 and 155.5±10.4 ml/100 g/min, respectively), TGN-020 produced a significant increase in rCBF compared with saline-treated WT mice (control), reaching a plateau 20 min after administration (118.45±8.13%, $P<0.01$). TGN-020 showed no effect on KO mice, supporting the concept that the observed increase in rCBF in WT mice was AQP-4 dependent. Administration of acetazolamide (positive control) produced an even greater increase in rCBF in WT compared with TGN-020 and a similar response in KO mice as well, reaching a sustained plateau 5 min after administration (138.50±9.75 and 138.52±9.76%, respectively, $P<0.01$ compared with baseline or saline-treated control mice). The study demonstrated that AQP-4 plays a role in regulation of rCBF. *NeuroReport* 00:000–000 © 2013 Wolters Kluwer Health | Lippincott Williams & Wilkins.

NeuroReport 2013, **00**:000–000

Keywords: acetazolamide, aquaporin, regional cerebral blood flow, TGN-020

[a]Center for Integrated Human Brain Science, Brain Research Institute, University of Niigata, Niigata, Japan and [b]Department of Neurology, University of California, Davis, California, USA

Correspondence to Tsutomu Nakada, MD, PhD, FAAN, Center for Integrated Human Brain Science, Brain Research Institute, University of Niigata,1-757 Asahimachi, Niigata 951-8585, Japan
Tel: +81 25 227 0677; fax: +81 25 227 0822;
e-mail: tnakada@bri.niigata-u.ac.jp

Received 11 January 2013 **accepted** 3 February 2013

Introduction

The aquaporin (AQP) family is a large collection of integral membrane proteins that enable the movement of water and other small neutral solutes across biological membranes. So far, seven AQP isoforms have been identified in the mammalian central nervous system (CNS) by reverse transcription PCR. However, only three isoforms, namely AQP-1, AQP-4, and AQP-9, have been identified *in vivo* [1]. AQP-4 represents the most abundant isoform located in astroglial cells lining the ependymal and pial surfaces [2]. AQP-1 is expressed in the choroid plexus epithelium [3]. In contrast to capillaries in the body, AQP-1 in CNS capillaries have actively suppressed [4]. AQP-9 is a water, glycerol, and lactate permeable isoform that is only scarcely expressed in the CNS [1]. Although it is conceivable that AQP-1 plays a role in production of cerebrospinal fluid and that AQP-9 has only limited function in the CNS, the physiological role of the most abundant isoform, AQP-4, remains unclear despite evidence implicating AQP-4 in the pathogenesis of various brain diseases, from autism to multiple sclerosis and Alzheimer's disease [5–8].

Using brain slice preparation, we have previously demonstrated that neural activity induced morphological changes, believed to reflect a reduction in extracellular space secondary to astrocyte swelling, which are significantly reduced in AQP-4 knockout (KO) mice [9]. As neural activities-induced astrocyte swelling has consistently been shown to coincide with in-vivo brain activation as detected by functional MRI, this observation strongly suggests that AQP-4 may play an important role in the genesis of the physiological alteration associated with brain activation, especially that of neural flow coupling [10]. Accordingly, we examined the effects of the AQP-4 inhibitor TGN-020 on cerebral blood flow (CBF) *in vivo* in AQP-4 KO and wild-type (WT) mice.

Materials and methods

The study was carried out in accordance with the animal research guidelines of the Internal Review Board of University of Niigata. AQP-4 KO mice were produced by homologous recombination using an embryonic stem cell line from the C57BL/6 strain as described previously [9].

Measurement of baseline absolute regional cerebral blood flow by magnetic resonance imaging

Baseline absolute regional cerebral blood flow (rCBF) of WT and KO mice (male and female, 8–12 weeks old, $n = 5$ for each group) was measured using MRI with a 15 cm bore, 7 T horizontal magnet (Magnex Scientific, Abingdon, UK), using a Varian Unity-INOVA-300 system (Varian Inc., Palo Alto, California, USA) equipped with an actively shielded gradient. A custom designed eight element, ϕ40 mm birdcage coil was used for radiofrequency transmission.

Spontaneously breathing mice were anesthetized using urethane (1.2 g/kg, intraperitoneally). The following anesthesia protocol was used to avoid respiratory depression. Urethane, 600 mg/kg, was administered intraperitoneally at $t = 0$; two additional doses of urethane, 300 mg/kg, were

0959-4965 © 2013 Wolters Kluwer Health | Lippincott Williams & Wilkins DOI: 10.1097/WNR.0b013e32835fc827

administered subsequently 10 and 20 min after the first dose. Mice were placed on their back in a custom designed Plexiglas stereotactic holder, and the head was immobilized using ear and tooth bars. The rectal temperature was maintained at 37 ± 0.5°C using a temperature control system. Oxygen saturation (SpO_2) was monitored throughout the study procedure using a pulse oximeter, Mouse Ox (STARR Life Sciences Co., Oakmont, Pennsylvania, USA), with probe placement on the left thigh.

The cerebral perfusion images were measured using continuous arterial spin labeling [11] with centric ordered snapshot-FLASH. The adiabatic inversion for inflowing arterial protons was accomplished with an axial gradient of 428.5 Hz/mm and continuous radiofrequency transmission of ~600 Hz at a frequency offset of ±4285 Hz alternatingly from the imaging slab and mirror plane. This protocol placed the inversion plane at ±10 mm from the imaging plane (Fig. 1a and c. After a 2-s inversion period, a 500 ms delay was set to eliminate the effect of regional transit time delay [12]. Imaging parameters of the pulse sequence were as follows: repetition time (TR)/echo time 4/2 ms; TR 5 s; field of view 20 × 20 mm; slice thickness 2 mm; and matrix size 128 × 64. A total of 64 image pairs were summated to improve the signal-to-noise ratio.

Magnetization transfer was measured with the identical conditions as for the cerebral perfusion measurement but without the axial gradient for adiabatic inversion. Measurement of T1 was accomplished using a centric ordered snapshot-FLASH with a hyperbolic secant inversion pulse, 64-point inversion delay (100–6400 ms), and 10 s TR.

Quantitative rCBF maps ($n = 5$ for each group) were calculated from the cerebral perfusion images, T1 maps, and magnetization transfer maps, according to the method described by Ewing *et al.* [13]. The rCBF maps were computed using an image preparing software (MR Vision; MR Vision Co., Menlo Park, California, USA) on a Linux Workstation (Dell, Round Rock, Texas, USA). A region of interest (ROI) of ~3 × 4 mm was set to the cortical surface (Fig. 1b).

Fig. 1

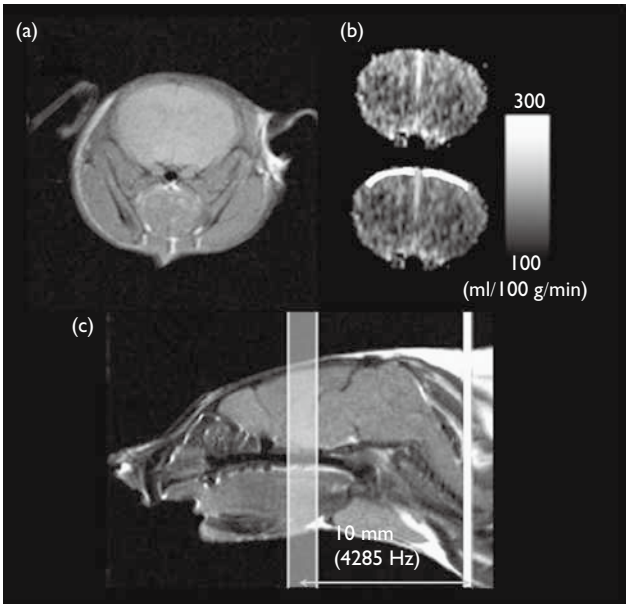

Baseline absolute rCBF in WT and KO mice. An anatomical (a) and absolute rCBF MRI (b) of a WT mouse. The white line in the rCBF MRI [lower image, (b)] depicts the region of interest for rCBF comparison between WT and KO mice. Imaging slabs were set to 6 mm caudally from the top of the cerebrum, which is ~3 mm caudal from the bregma. Adiabatic inversion pulses were irradiated onto the axial plane 10 mm caudally from the imaging slab and mirror plane alternatingly (c). KO, knockout; rCBF, regional cerebral blood flow; WT, wild type.

Measurement of relative regional cerebral blood flow in study condition

The relative rCBF was determined using laser speckle flowmetry (Omegazone, Laser Speckle Blood Flow Imager; Omegawave, Tokyo, Japan), which obtains high-resolution two-dimensional images every 0.3 s [14]. A 780 nm laser illuminated the area of interest, and scattered light was scanned with a charge-coupled device camera. The resulting imaging data was then transferred to a computer for analysis. Five scans (1.5 s) were signal-averaged to give 91 × 68 pixel images, each having an imaging field of view of 24 × 18 mm. These images were saved to the computer for further analysis. For rCBF analysis, a ROI of ~3 × 4 mm was set on the left parietal and left frontal cortex, positioning the center of ROI 3 mm caudally and 2 mm laterally from the bregma and within an area delimited by the superior sagittal sinus, superior anastomotic vein (vein of Trolard), and main superior cerebral vein, just caudal to the superior anastomotic vein. ROIs were manually selected to avoid large surface arteries or veins (Fig. 2a). rCBF was calculated by averaging 80 images (120 s) over 5 min, and values were normalized to baseline rCBF.

WT and KO mice (male and female, 8–12 weeks old, $n = 18$ each) were used for the studies. Animals were anesthetized with an intraperitoneal administration of urethane (1.2 g/kg). The scalp was removed to allow rCBF changes to be visualized through the bone. The exposed skull was covered with a mixture of petroleum jelly and glycerin (1 : 1) to prevent the surface from drying out. For imaging studies, the head was fixed in a stereotactic device. Head and rectal temperatures were kept at 37.0 ± 0.5°C throughout the experiment using a custom designed cooling system and heating pad. SpO_2 was monitored throughout the study procedure, and data from the animals showing SpO_2 of less than 93% at any point during the experiment were discarded (two KO and one WT), a criterion described previously [15]. After a 30 min stabilization period, measurements of baseline rCBF were recorded for 5 min. Subsequently, mice received TGN-020 intraperitoneally (200 mg/kg, in 0.2 ml isotonic saline, $n = 5$ each for WT and KO). The positive control mice ($n = 5$ each for both WT and KO) were administered acetazolamide (50 mg/kg)

Fig. 2

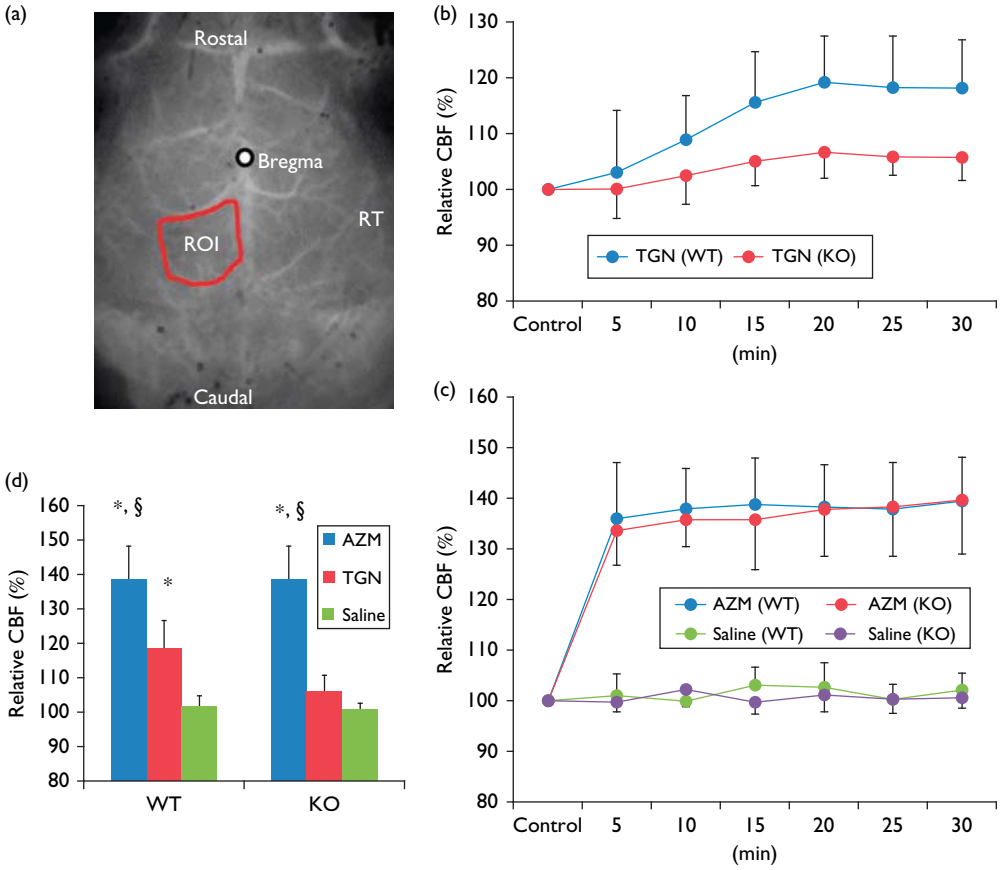

The rCBF response after drug administration. The center of the ROI was set at 3 mm caudally and 2 mm laterally from the bregma (marked by ○) (a). The time course of rCBF changes in WT mice (b) shows a significant increase in rCBF associated with TGN-020 administration, although less than that observed after AZM administration (positive control). Note that for the KO mice, there is no TGN-020-associated rCBF increase, whereas AZM (positive control) induced a significant increase (c). Average rCBF changes after reaching a plateau (15–30 min after drug administration) (d). The error bar indicates SD. AZM, acetazolamide; CBF, cerebral blood flow; KO, knockout; rCBF, regional cerebral blood flow; ROI, region of interest; RT, right side of the brain; TGN, TGN-020; WT, wild type. *$P<0.01$ vs. saline, $^{\S}P<0.01$ vs. TGN-020 (Fisher's PLSD test).

dissolved in 0.2 ml isotonic saline intraperitoneally, and negative control mice ($n = 5$ each for both WT and KO) were administered an identical volume of isotonic saline intraperitoneally. The rCBF was then measured continuously for 30 min after administration.

To avoid CBF instability due to arterial blood gas (ABG) sampling, assessment for changes in ABG values before and after drug administration were studied separately in another 20 mice ($n = 10$ each for WT and KO mice: five for TGN-020 administration and five for acetazolamide administration) under experimental conditions identical to those for the CBF response study. The ABGs were sampled twice per animal, once before and once after administration of TGN-020 or acetazolamide. The sample volume was 0.15 ml.

Statistical procedure

Numerical data were subjected to Student's *t*-test for group analysis of baseline CBF and analysis of variance with Fisher's post-hoc test to compare rCBF responses against drug administration for the six groups (TGN-020, acetazolamide, and saline administration groups for both WT and KO mice); a *P* value less than 0.05 was regarded as statistically significant. All data are shown as mean ± SD.

Results

Baseline absolute rCBF in the surface cerebral cortex was similar for both WT and KO mice (158.9 ± 17.7 and 155.5 ± 10.4 ml/100 g/min, respectively) (Fig. 1d).

In the rCBF response study animals, the ABGs remained within physiological range, except after the administration of acetazolamide, which evoked acidosis due to CO_2 retention (Table 1).

Administration of TGN-020 resulted in a significant increase in rCBF, reaching a plateau 20 min after administration in WT mice, 118.45 ± 8.13% ($P < 0.01$), as compared with saline-treated negative control mice

(Fig. 2c and d, left). There was no significant increase in rCBF after TGN-020 administration in KO mice (Fig. 2b and d, right), confirming that the observed rCBF increase in WT mice was AQP-4 dependent. Administration of acetazolamide (positive control) resulted in an even greater increase in rCBF in WT mice, and a similar increase was observed in KO mice, reaching a plateau 5 min after administration, which lasted 25 min in both WT and KO mice (138.50±9.75 and 138.52±9.76%, respectively) ($P < 0.01$) compared with saline-treated negative control mice (Fig. 2b and d).

Discussion

TGN-020, 2-nicotinamido-1,3,4-thiadiazole, was identified on the basis of conserved physicochemical features of several known drugs found to inhibit AQP-4 water transport *in vitro*. TGN-020 was found to inhibit water transport through human AQP-4-M23 with an IC_{50} equal to 3 μM and 73% maximum inhibition [16,17]. Subsequently, using ^{11}C-labeled TGN-020 and PET, we demonstrated that the affinity of TGN-020 for AQP-4, *in vivo*, followed a specific brain distribution pattern [18]. The effect of AQP-4 inhibition by TGN-020 in preventing brain edema was demonstrated in a rodent model of cerebral ischemia *in vivo* [15]. The present study demonstrated another in-vivo effect of TGN-020 on AQP-4 inhibition, namely an increase in rCBF and, thereby, demonstrating that AQP-4 plays a role in regulation of rCBF.

Table 1 Changes in arterial blood gases before and after drug administration

	TGN ($n=5$)		AZM ($n=5$)	
	Pre	15 min	Pre	15 min
pH				
WT	7.41±0.024	7.40±0.020	7.41±0.021	7.27±0.058
KO	7.43±0.015	7.40±0.025	7.43±0.022	7.27±0.030
CO_2 (mmHg)				
WT	38.8±2.28	36.8±1.30	39.6±2.40	56.6±4.10
KO	41.6±1.52	38.2±3.42	40.8±2.72	57.4±4.67
O_2 (mmHg)				
WT	96.8±7.36	99.6±7.67	97.6±7.37	101±6.08
KO	92.4±2.70	98.8±6.76	94.8±5.22	104±9.82

AZM, acetazolamide; KO, knockout mice; TGN, TGN-020; WT, wild-type mice.

Increased rCBF associated with brain activation is a well-recognized phenomenon. Nevertheless, to date, the precise mechanism underlying the observed neural flow coupling phenomenon has remained elusive. As an increase in rCBF associated with neural activities is a microenvironmental, not a macroenvironmental, event occurring within an area limited to 250 μm around the site of the neural activity [19], the regulatory mechanism is likely within the capillaries, rather than within vessels containing muscles, such as arterioles or arteries, the tone of which can indeed be regulated effectively. Furthermore, in addition to an increase in rCBF, neural activity induces astrocyte swelling. Such swellings are significantly reduced in AQP-4 KO mice [9]. Altogether, the experimental evidence argues that regulation of water contents in the pericapillary extracellular space by astrocyte AQP-4 may control rCBF associated with neural activities (Fig. 3). In the brain, AQP-1 expression within

Fig. 3

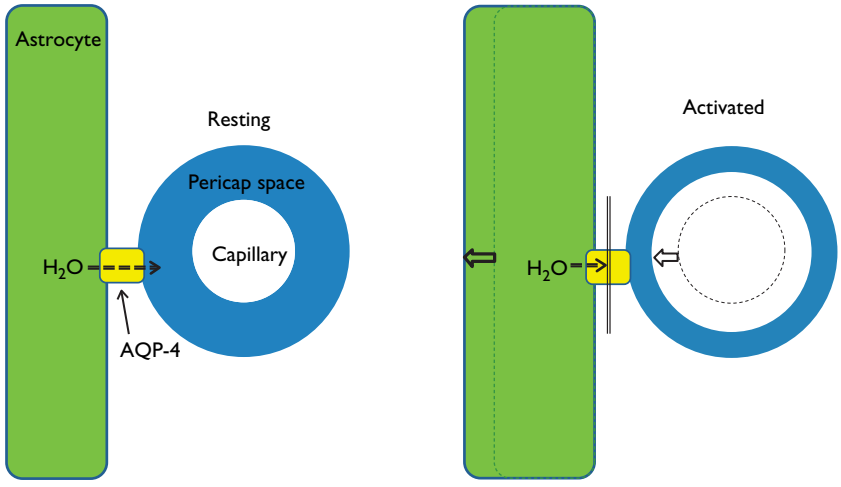

Schematic presentation of the hypothesis. Neural activity is known to produce two distinctive phenomena, namely astrocyte swelling and increased rCBF. As an increase in rCBF associated with neural activities occurs within an area limited to 250 μm around the site of the neural activity, it is very likely to be a phenomenon associated with capillaries. The present study clearly demonstrates that inhibition of AQP-4 effectively increased rCBF. The hypothesis is schematically presented here: inhibition of AQP-4 results in blockage of water flow from the astrocyte into the pericapillary space (pericap space). This in turn results in astrocyte swelling and capillary expansion due to reduction of the pericapillary space. The process associated with brain activation can be explained in the same manner. AQP-4, aquaporin-4; rCBF, regional cerebral blood flow.

capillaries is naturally, actively suppressed, a condition that also supports the concept that a regulatory control mechanism of water contents within the pericapillary space by astrocytes may be an important factor for maintaining neural function, if not for the proper maintenance of the blood–brain barrier.

Acetazolamide has consistently been found to increase rCBF in the normal brain, the underlying mechanism of which is so far unknown. Along with the fact that carbonic anhydrase (CA) is the enzyme that deals not only with CO_2, HCO_3^-, and H^+ but also with H_2O, the current study suggests that a new concept on the effect of acetazolamide with respect to water homeostasis is also called for. The isoforms of CA present in the brain are cytosolic CA II and membrane-bound CA IV. CA II is localized to the choroid plexus and oligodendroglia, whereas CA IV is found in the capillaries [20]. AQP-1 is also highly expressed in the choroid plexus [3]. However, AQP-1, which is usually significantly expressed in capillaries, is naturally, actively suppressed in brain capillaries [4]. It appears that these specific arrangements in the brain are necessary to maintain proper functionality of the blood–brain barrier, and at the same time, to ensure production of cerebrospinal fluid in the choroid plexus.

CA IV is expressed on the luminal surface of brain capillaries [20]. Similarly, CA IV is also expressed on the luminal surface of pulmonary capillaries and of proximal renal tubules [21], which are the two main sites of acid–base balance control accomplished through the regulation of total body contents of CO_2 and/or HCO_3^-. Although it remains speculative, CA IV may be the form of CA specialized for controlling CO_2 and/or HCO_3^- at the specific site at which controlling water content is crucial. Suppression of CA IV in the brain capillaries by acetazolamide may result in alteration of water contents within the space, affecting rCBF similar to AQP-4 inhibition.

Conclusion

We have demonstrated that AQP-4, an isoform of the water channel AQP family, abundantly expressed in the brain and distributed specifically along the subpial and pericapillary end-feet of astrocytes, plays a significant role in controlling rCBF. The study demands a new directionality in the investigation of neural activity-induced rCBF changes, a response known as neural flow coupling.

Acknowledgements

The work was supported by grants from the Ministry of Education, Culture, Sports, Science and Technology (Japan) and the University of Niigata.

Conflicts of interest

There are no conflicts of interest.

References

1 Badaut J, Brunet JF, Regli L. Aquaporins in the brain: from aqueduct to 'multi-duct'. *Metab Brain Dis* 2007; **22**:251–263.
2 Mobasheri A, Marples D, Young IS, Floyd RV, Moskaluk CA, Frigeri A. Distribution of the AQP4 water channel in normal human tissues. *Channels* 2007; **1**:29–38.
3 Nielsen S, Smith BL, Christensen EI, Agre P. Distribution of the aquaporin CHIP in secretory and resorptive epithelia and capillary endothelia. *Proc Natl Acad Sci USA* 1993; **90**:7275–7279.
4 Dolman D, Drndarski S, Abbott NJ, Rattray M. Induction of aquaporin 1 but not aquaporin 4 messenger RNA in rat primary brain microvessel endothelial cells in culture. *J Neurochem* 2005; **93**:825–833.
5 Kimelberg HK, Ransom BR. Physiological and pathological aspects of astrocytic swelling. In: Federoff S, Vernadakis A, editors. *Astrocytes. Cell biology and pathology of astrocytes*. San Diego, CA: Academic Press; 1986. pp. 77–127.
6 Fatemi SH, Folsom TD, Reutiman TJ, Lee S. Expression of astrocytic markers aquaporin 4 and connexin 43 is altered in brains of subjects with autism. *Synapse* 2008; **62**:501–507.
7 Benarroch EE. Clinical implications of neuroscience research. Aquaporin-4, homeostasis, and neurologic disease. *Neurology* 2007; **69**:2266–2268.
8 Yang J, Lunde LK, Nuntagij P, Oguchi T, Camassa LM, Nilsson LN, *et al.* Loss of astrocyte polarization in the tg-ArcSwe mouse model of Alzheimer's disease. *J Alzheimers Dis* 2011; **27**:711–722.
9 Kitaura H, Tsujita M, Huber VJ, Kakita A, Shibuki K, Sakimura K, *et al.* Activity-dependent glial swelling is impaired in aquaporin-4 knockout mice. *Neurosci Res* 2009; **64**:208–212.
10 Figley CR, Leitch JK, Stroman PW. In contrast to BOLD: signal enhancement by extravascular water protons as an alternative mechanism of endogenous fMRI signal change. *Magn Reson Imaging* 2010; **28**:1234–1243.
11 Williams DS, Detre JA, Leigh JS, Koretsky AP. Magnetic resonance imaging of perfusion using spin inversion of arterial water. *Proc Natl Acad Sci USA* 1992; **89**:212–216.
12 Alsop DC, Detre JA. Reduced transit-time sensitivity in noninvasive magnetic resonance imaging of human cerebral blood flow. *J Cereb Blood Flow Metab* 1996; **16**:1236–1249.
13 Ewing JR, Wei L, Knight RA, Pawa S, Nagaraja TN, Brusca T, *et al.* Direct comparison of local cerebral blood flow rates measured by MRI arterial spin-tagging and quantitative autoradiography in a rat model of experimental cerebral ischemia. *J Cereb Blood Flow Metab* 2003; **23**:198–209.
14 Miller D, Forrester K, Leonard C, Salo P, Bray RC. ACL deficiency impairs the vasoconstrictive efficacy of neuropeptide Y and phenylephrine in articular tissues: a laser speckle perfusion imaging study. *J Appl Physiol* 2005; **98**:329–333.
15 Igarashi H, Huber VJ, Tsujita M, Nakada T. Pretreatment with a novel aquaporin 4 inhibitor, TGN-020, significantly reduces ischemic cerebral edema. *Neurol Sci* 2011; **32**:113–116.
16 Huber VJ, Tsujita M, Nakada T. Identification of aquaporin 4 inhibitors using in vitro and in silico methods. *Bioorg Med Chem* 2009; **17**:411–417.
17 Huber VJ, Tsujita M, Kwee IL, Nakada T. Inhibition of aquaporin 4 by antiepileptic drugs. *Bioorg Med Chem* 2009; **17**:418–424.
18 Nakamura Y, Suzuki Y, Tsujita M, Huber VJ, Yamada K, Nakada T. Development of a novel ligand, [^{11}C]TGN-020, for aquaporin 4 positron emission tomography imaging. *ACS Chem Neurosci* 2011; **2**:568–571.
19 Silver IA. Cellular microenvironment in relation to local blood flow. In: Elliott K, O'Connor Maeve, editors. *Ciba Foundation Symposium 56 – cerebral vascular smooth muscle and its control. Chapter 5*. Chichester, UK: John Wiley & Sons; 2008. pp. 49–67.
20 Ghandour MS, Langley OK, Zhu XL, Waheed A, Sly WS. Carbonic anhydrase IV on brain capillary endothelial cells: a marker associated with the blood–brain barrier. *Proc Natl Acad Sci USA* 1992; **89**:6823–6827.
21 Sterling D, Alvarez BV, Casey JR. The extracellular component of a transport metabolon. Extracellular loop 4 of the human AE1 Cl-/HCO3-exchanger binds carbonic anhydrase IV. *J Biol Chem* 2002; **277**:25239–25246.